COMPDYN 2011
3^{rd} ECCOMAS Thematic Conference on
Computational Methods in Structural Dynamics and Earthquake Engineering
M. Papadrakakis, M. Fragiadakis, V. Plevris (eds.)
Corfu, Greece, 25-28 May 2011

NONCLASSICAL MODELS IN THE SHELL THEORY WITH APPLICATIONS TO MULTILAYERED NANOTUBES

Svetlana M. Bauer, Andrei M. Ermakov, Stanislava V. Kashtanova, Nikita F. Morozov[1]

[1] St. Petersburg State University, St. Petersburg, Russia
s_bauer@mail.ru, khopesh_ra@mail.ru, kastasya@yandex.ru, morozov@nm1016.spb.edu

Keywords: Theory of anisotropic shells, Shell theory of Paliy-Spiro, Shell theory of Rodionova-Titaev-Chernykh.

Abstract. *In [1] the stiffness of bridges and cantilevers made of natural chrysotile asbestos nanotubes has been studied by means of scanning probe microscopy. The stiffness is defined as a ratio the value of local load (applied to the tube) to the value of the displacement. The nanotubes with different materials for fillings are analyzed. The experiments show that the stiffness of the tube depends on the materials for filling. The tubes with water are softer than the tubes without filling materials and the tubes filled with mercury are more rigid than tubes without filling materials. It was shown in [1] that the classical theory of beam bending can not explain the experimental results, but the experimental results well agree with the Timoshenko-Reissner theory (at least qualitatively), when interlaminar shear modulus of elasticity changes for different filling materials. When additional factors such as lamination of structure and cylindrical anisotropy are taken into account [2] the theory of Rodionova-Titaev-Chernykh (RTC) permits to obtain much more reliable results. In this work the authors also applied one more nonclassical shell theory, namely the shell theory of Paliy-Spiro (PS) developed for medium - thickness shells and considered radial pressure. The comparison of nonclassical shell theories (RTC and PS) with experimental data and FEM calculations are presented in the report.*

1 INTRODUCTION

It is known [3] that mechanical characteristics corresponding to nano-dimensional structure elements such as beams, plates and shells can differ from mechanical characteristics corresponding to structures of the same material, which have "normal" geometrical sizes. There is a possibility of appearance of the anisotropy of nanoobjects. In [1], [2] results of experiments, which examined mechanical properties of nanotubes made of natural chrysolite asbestos are discussed. The diameter of nanotubes is approximately equal to 30nm, internal diameter is 5nm. The inner cavity of a tube was filled with water, mercury or tellurium under pressure. The rigidity of nanotubes was measured with the use of scanning probing microscopy. The rigidity was understood as the ratio between applied strain and value of bridge deflection formed by the nanotube, which blocked an opening in porous bottom layer. (Conditions of the experiment are described in detail in [1]). The experiments showed that tube filled with water is substantially softer than a "dry" tube (tube without any filler) and tubes filled with mercury are slightly more rigid than "dry" tubes. In [1] experimental data and the results of modeling were compared. The simplest classical models of isotropic beams and non-classical transversal isotropic models were considered. In [2] the problem of nanotubes deformation was solved with the use of the Rodionova-Titaev-Chernykh (RTCH) theory of anisotropic shells [4] , which permits to take into account layered structure of asbestos and cylindrical anisotropy as well. In this work deformation of a multilayered tube under locally applied load (Fig. 1) is found with the use of the theory of anisotropic shells of moderate thickness, which is developed in [5]. There was made a comparison of the results obtained with the use of the Timoshenko-Reissner (TR) theory [6] , RTCH theory, the Paliy-Spiro theory and FEM calculations in ANSYS code.

2 PROBLEM DEFINITION

Let α and β be cylindrical coordinates on a shell surface, α — the polar angle, β — coordinate along the tube's generatrix, $h^{(i)}$ — thicknesses, $R^{(i)}$ — radiuses of medium surfaces of the shell layers, and L — tube's length. For definition of coefficients we will use symbol $A_j^{(i)}$. Low index j denotes curvilinear coordinate corresponding to the value A, upper index i — denotes to which layer it corresponds, i.e. if $i = 1$ then A corresponds to the first inner layer, if $i = N$ then A corresponds to the last outer layer. $E_1^{(i)}, E_2^{(i)}, E_3^{(i)}$ are modules of elasticity in tangential and normal directions, $\nu_{jk}^{(i)}$ are the Poisson's ratios.

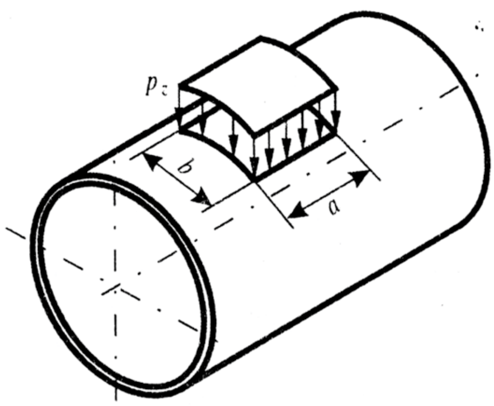

Figure 1: Geometrical model of the tube

We studies the stress-strain state of a multilayered tube under locally applied load with the use of the new improved iterative theory of anisotropic shells of Rodionova-Titaeva-Chernykh [4], the theory by Paliy-Spiro suggested in [5], the Timoshenko-Reissner theory.

The improved iterative RTCH theory is based on the following hypotheses:

1. transverse tangential and normal stresses are distributed on shell's thickness according to quadratic and cubic laws respectively;

2. tangential and normal components of the displacement vector are distributed on the shell thickness according to quadratic and cubic laws respectively.

This theory takes into account turns of fibers, their deviation and change of their length.

Functions which describe displacement of the shell's layer $u_1(\alpha,\beta,z)$, $u_2(\alpha,\beta,z)$, $u_3(\alpha,\beta,z)$ according to the Rodionova-Chernykh theory are suggested to be found as series of Legendre polynomials $P_0,\ P_1,\ P_2,\ P_3$ in normal coordinate $z \in \left[-\frac{h}{2}, \frac{h}{2}\right]$

$$\begin{aligned} u_1(\alpha,\beta,z) &= u(\alpha,\beta)P_0(z)+\gamma_1(\alpha,\beta)P_1(z)+\theta_1(\alpha,\beta)P_2(z)+\varphi_1(\alpha,\beta)P_3(z), \\ u_2(\alpha,\beta,z) &= v(\alpha,\beta)P_0(z)+\gamma_2(\alpha,\beta)P_1(z)+\theta_2(\alpha,\beta)P_2(z)+\varphi_2(\alpha,\beta)P_3(z), \\ u_3(\alpha,\beta,z) &= w(\alpha,\beta)P_0(z)+\gamma_3(\alpha,\beta)P_1(z)+\theta_3(\alpha,\beta)P_2(z), \end{aligned} \tag{1}$$

$$P_0(z)=1, \quad P_1(z)=\frac{2z}{h}, \quad P_2(z)=\frac{6z^2}{h^2}-\frac{1}{2}, \quad P_3(z)=\frac{20z^3}{h^3}-\frac{3z}{h}, \tag{2}$$

where u, v, w are the components of the displacement vector for points of the middle surface of the shell, γ_3 and θ_3 characterize change in length of the normal to this surface, γ_1 and γ_2 are angles of rotation of the normal in planes $(\alpha,z),(\beta,z)$ correspondingly. The variables θ_1 and φ_1, describe normal curvature of the fiber in plane (α,z), quantities θ_2 φ_2, normal curvature in plane (β,z) before deformation they were perpendicular to the shell middle surface.

The Paliy-Spiro shells theory [5] is a theory of shells of moderate thickness, which assumes the following hypotheses:

1. straight fibers of the shell, which are perpendicular to its middle surface before deformation, remain also straight after deformation;

2. cosine of the slope angle of these fibers shell's slope to the middle surface of the deformed shell is equal to the averaged angle of transverse shear.

Mathematical formulation of these hypotheses gives following equalities:

$$\begin{aligned} &u_1(\alpha,\beta,z)=u(\alpha,\beta)+\phi(\alpha,\beta)z, && u_2(\alpha,\beta,z)=v(\alpha,\beta)+\psi(\alpha,\beta)z, \\ &u_3(\alpha,\beta,z)=w(\alpha,\beta)+F(\alpha,\beta,z), && \\ &\phi(\alpha,\beta)=\gamma_1(\alpha,\beta)+\phi_0(\alpha,\beta), && \psi(\alpha,\beta)=\gamma_2(\alpha,\beta)+\psi_0(\alpha,\beta), \\ &\phi_0(\alpha,\beta)=-\frac{1}{A_1}\frac{\partial w(\alpha,\beta)}{\partial\alpha}+k_1u(\alpha,\beta), && \psi_0(\alpha,\beta)=-\frac{1}{A_2}\frac{\partial w(\alpha,\beta)}{\partial\alpha}+k_2v(\alpha,\beta), \end{aligned} \tag{3}$$

where ϕ and ψ are angles of normal's rotation in planes $(\alpha,z),(\beta,z)$; ϕ_0, ψ_0,γ_1 and γ_2 — are angles of normal's rotation to the median surface and angles of displacement in the same planes. The function $F(\alpha,\beta,z)$ characterizes change of length of the normal to the median surface.

The Lamé's coefficients and curvature coefficients, which determine geometry of the cylindrical shell have the following form

$$A_1^{(i)}=R^{(i)}, \quad A_2^{(i)}=1, \quad k_1^{(i)}=\frac{1}{R^{(i)}}, \quad k_2^{(i)}=0 \tag{4}$$

Let us introduce the following dimensionless variables:

$$\begin{aligned}
&\tilde{R}^{(i)} = \frac{A_1^{(i)}}{A_2^{(i)}}, \quad \tilde{h}^{(i)} = \frac{h}{R^{(i)}}, \\
&\left\{\tilde{u}^{(i)}, \tilde{v}^{(i)}, \tilde{w}^{(i)}, \tilde{\gamma}_{1,2,3}^{(i)}, \tilde{\theta}_{1,2,3}^{(i)}, \tilde{\varphi}_{1,2}^{(i)}, \tilde{\phi}_{,0}^{(i)}, \tilde{\psi}_{,0}^{(i)}\right\} \\
&= \frac{1}{h}\left\{u^{(i)}, v^{(i)}, w^{(i)}, \gamma_{1,2,3}^{(i)}, \theta_{1,2,3}^{(i)}, \varphi_{1,2}^{(i)}, \phi_{,0}^{(i)}, \psi_{,0}^{(i)}\right\}, \\
&\tilde{E}_{2,3} = \frac{E_{2,3}}{E_1}, \quad \tilde{G}_{13,12,23} = \frac{G_{13,12,23}}{E_1}, \\
&\tilde{Pin}_{1,2,3}{}^{(i)} = \frac{Pin_{1,2,3}^{(i)}}{E_1}, \ \tilde{Pout}_{1,2,3}{}^{(i)} = \frac{Pout_{1,2,3}^{(i)}}{E_1}, \\
&\left\{\tilde{T}_{0,1,2}^{(i)}, \tilde{Q}_{1,2}^{(i)}, \tilde{m}_{1,2,3}^{(i)}\right\} = \frac{\left\{T_{0,1,2}^{(i)}, Q_{1,2}^{(i)}, m_{1,2,3}^{(i)}\right\}}{R^{(i)}E_1}, \\
&\left\{\tilde{M}_{0,1,2}^{(i)}\right\} = \frac{\left\{M_{0,1,2}^{(i)}\right\}}{R^{(i)}E_1 h}, \left\{\tilde{q}_{1,2,3}^{(i)}\right\} = \frac{\left\{q_{1,2,3}^{(i)}\right\}}{E_1},
\end{aligned} \tag{5}$$

where $Pout_x$, Pin_x are the values of the pressure on the internal and external shell surfaces. For simplicity we introduce the following parameters:

$$\begin{aligned}
&E_{11} = \frac{1}{1-\nu_{12}\nu_{21}}, \quad E_{12} = \frac{\tilde{E}_2}{1-\nu_{12}\nu_{21}}, \quad E_{22} = \frac{\nu_{12}}{1-\nu_{12}\nu_{21}}, \\
&E_z = \frac{\tilde{E}_3}{1-\nu_{13}\mu_1-\nu_{23}\mu_2}, \quad \mu_1 = \frac{\nu_{31}+\nu_{21}\nu_{32}}{1-\nu_{12}\nu_{21}}, \quad \mu_2 = \frac{\nu_{32}+\nu_{21}\nu_{31}}{1-\nu_{12}\nu_{21}}, \\
&K_{11} = -E_{11}\tilde{h}^{(i)}, \quad K_{12} = E_{22}\tilde{h}^{(i)}, \quad K_{21} = \frac{3}{2}E_{11}\tilde{h}^{(i)}\mu_1, \quad K_{22} = \frac{3}{2}E_{22}\tilde{h}^{(i)}\mu_2, \\
&K_{13} = E_{11}\frac{\tilde{h}^{(i)}}{2}(\mu_2+2\nu_{12}\mu_1), \quad K_{23} = E_{11}\frac{\tilde{h}^{(i)}}{2}(\nu_{12}\mu_1+2\mu_2), \\
&\tilde{m}_x^{(i)} = \frac{\tilde{h}^{(i)}}{2}\tilde{Pout}_x{}^{(i)}\left(1+\frac{\tilde{h}^{(i)}}{2}\right) + \frac{\tilde{h}^{(i)}}{2}\tilde{Pin}_x{}^{(i)}\left(1-\frac{\tilde{h}^{(i)}}{2}\right), \quad (x=1,2,3), \\
&\tilde{q}_x^{(i)} = \tilde{Pout}_x{}^{(i)}\left(1+\frac{\tilde{h}^{(i)}}{2}\right) - \tilde{Pin}_x{}^{(i)}\left(1-\frac{\tilde{h}^{(i)}}{2}\right), \quad (x=1,2,3)
\end{aligned} \tag{6}$$

3 CORRELATIONS OF THE RODIONOVA-TITAEV-CHERNYKH SHELL THEORY AND THE PALIY-SPIRO THEORY

Shell deformations of the theories under consideration are expressed through the components of displacements with the use of the following equations.

Deformation components those are different for the theories are underlining. Below we present the relations for moments, strains and deformation components for the RTCH theory, which were converted for the case of a cylindrical shell. Substituting the given dependencies in expression (7), we can receive an equation, which characterizes their connection to components of the displacement.

Rodionova-Titaev-Chernykh theory	Paliy-Spiro theory
$\tilde\varepsilon_1^{(i)} = \tilde h^{(i)}(\frac{\partial \tilde u^{(i)}}{\partial \alpha^{(i)}} + \tilde w^{(i)}), \quad \tilde\varepsilon_2^{(i)} = \frac{\partial \tilde v^{(i)}}{\partial \beta^{(i)}},$	$\tilde\varepsilon_1^{(i)} = \tilde h^{(i)}(\frac{\partial \tilde u^{(i)}}{\partial \alpha^{(i)}} + \tilde w^{(i)}), \quad \tilde\varepsilon_2^{(i)} = \frac{\partial \tilde v^{(i)}}{\partial \beta^{(i)}},$
$\tilde\eta_1^{(i)} = \tilde h^{(i)}(\frac{\partial \tilde\gamma_1^{(i)}}{\partial \alpha^{(i)}} + \tilde\gamma_3^{(i)}), \quad \tilde\eta_2^{(i)} = \frac{\partial \tilde\gamma_2^{(i)}}{\partial \beta^{(i)}},$	$\underline{\tilde\eta_1^{(i)} = \tilde h^{(i)}(\frac{\partial \tilde\phi^{(i)}}{\partial \alpha^{(i)}})}, \quad \underline{\tilde\eta_2^{(i)} = \frac{\partial \tilde\psi^{(i)}}{\partial \beta^{(i)}}},$
$\tilde\varepsilon_{13}^{(i)} = \tilde h^{(i)} \frac{\partial \tilde w^{(i)}}{\partial \alpha^{(i)}} - \tilde h^{(i)} \tilde u^{(i)} + 2\tilde\gamma_1^{(i)},$	$\underline{\tilde\varepsilon_{13}^{(i)} = 0},$
$\tilde\varepsilon_{23}^{(i)} = \frac{\partial \tilde w^{(i)}}{\partial \beta^{(i)}} + 2\tilde\gamma_2^{(i)},$	$\underline{\tilde\varepsilon_{23}^{(i)} = 0},$
$\tilde\omega_1^{(i)} = \tilde h^{(i)} \frac{\partial \tilde v^{(i)}}{\partial \alpha^{(i)}}, \quad \tilde\omega_2^{(i)} = \frac{\partial \tilde u^{(i)}}{\partial \beta^{(i)}},$	$\tilde\omega_1^{(i)} = \tilde h^{(i)} \frac{\partial \tilde v^{(i)}}{\partial \alpha^{(i)}}, \quad \tilde\omega_2^{(i)} = \frac{\partial \tilde u^{(i)}}{\partial \beta^{(i)}},$
$\tilde\tau_1^{(i)} = \tilde h^{(i)} \frac{\partial \tilde\gamma_2^{(i)}}{\partial \alpha^{(i)}}, \quad \tilde\tau_2^{(i)} = \frac{\partial \tilde\gamma_1^{(i)}}{\partial \beta^{(i)}},$	$\underline{\tilde\tau_1^{(i)} = \tilde h^{(i)} \frac{\partial \tilde\psi^{(i)}}{\partial \alpha^{(i)}}}, \quad \underline{\tilde\tau_2^{(i)} = \frac{\partial \tilde\phi^{(i)}}{\partial \beta^{(i)}}},$
$\tilde\tau^{(i)} = \tilde\tau_1^{(i)} + \tilde\tau_2^{(i)}, \tilde\omega^{(i)} = \tilde\omega_1^{(i)} + \tilde\omega_2^{(i)}$	

Table 1: Deformation components in two theories

$$
\begin{aligned}
&\tilde T_1^{(i)} = E_{11}\tilde h^{(i)}\varepsilon_1^{(i)} + E_{12}\tilde h^{(i)}\varepsilon_2^{(i)} + \mu_1^{(i)}\tilde T_0^{(i)}, \tilde T_2^{(i)} = E_{12}\tilde h^{(i)}\varepsilon_1^{(i)} + E_{22}\tilde h^{(i)}\varepsilon_2^{(i)} + \mu_2^{(i)}\tilde T_0^{(i)},\\
&\tilde M_1^{(i)} = \tfrac{\tilde h^{(i)}}{6}(E_{11}\eta_1^{(i)} + E_{12}\eta_2^{(i)}) + \mu_1^{(i)}\tilde M_0^{(i)}, \tilde M_2^{(i)} = \tfrac{\tilde h^{(i)}}{6}(E_{12}\eta_1^{(i)} + E_{22}\eta_2^{(i)}) + \mu_2^{(i)}\tilde M_0^{(i)},\\
&\tilde T_{12}^{(i)} = \tilde T_{21}^{(i)} = \tilde G_{12}^{(i)}\tilde h^{(i)}\tilde\tau^{(i)}, \tilde M_{12}^{(i)} = \tilde M_{21}^{(i)} = \tfrac{1}{6}\tilde G_{12}^{(i)}\tilde h^{(i)}\tilde\omega^{(i)},\\
&\tilde Q_1^{(i)} = \tfrac{5\tilde h^{(i)}\tilde G_{13}^{(i)}}{6}\varepsilon_{13}^{(i)} + \tfrac{\tilde m_1^{(i)}}{6} - (\tilde h^{(i)})^2\tfrac{\tilde G_{13}^{(i)}}{6}\tfrac{\partial\theta_3^{(i)}}{\partial\alpha^{(i)}},\\
&\tilde Q_2^{(i)} = \tfrac{5\tilde h^{(i)}\tilde G_{23}^{(i)}}{6}\varepsilon_{23}^{(i)} + \tfrac{\tilde m_2^{(i)}}{6} - \tilde h^{(i)}\tfrac{\tilde G_{23}^{(i)}}{6}\tfrac{\partial\theta_3^{(i)}}{\partial\beta^{(i)}},\\
&\tilde T_0^{(i)} = \tilde m_3^{(i)} + \tfrac{(\tilde h^{(i)})^2}{12}\left(\tfrac{\partial\tilde q_1^{(i)}}{\partial\alpha^{(i)}} + \tilde R^{(i)}\tfrac{\partial\tilde q_2^{(i)}}{\partial\beta^{(i)}}\right) - \tilde h^{(i)}\tilde M_1^{(i)},\\
&M_0^{(i)} = \tfrac{(\tilde h^{(i)})^2}{10}\tilde q_3^{(i)} + \tfrac{\tilde h^{(i)}}{60}\left(\tfrac{\partial\tilde m_1^{(i)}}{\partial\alpha^{(i)}} + \tilde R^{(i)}\tfrac{\partial\tilde m_2^{(i)}}{\partial\beta^{(i)}}\right) - \tfrac{\tilde h^{(i)}}{60}\tilde T_1^{(i)}
\end{aligned}
\tag{7}
$$

Let us substitute the following relations (8) for six components of the displacement in formulas (7). Thus we reduce them to dependence on the five main components of the displacement $u, v, w, \gamma_1, \gamma_2$:

$$
\begin{aligned}
&\tilde\theta_1^{(i)} = \tfrac{\tilde q_1^{(i)}}{12G_{13}} - \tfrac{\tilde h^{(i)}}{6}\tfrac{\partial\tilde\gamma_3^{(i)}}{\partial\alpha^{(i)}}, && \tilde\varphi_1^{(i)} = \tfrac{{m_1}^{(i)} - \tilde Q_1^{(i)}}{10\tilde h^{(i)}\tilde G_{13}^{(i)}} - \tfrac{\tilde h^{(i)}}{10}\tfrac{\partial\tilde\theta_3^{(i)}}{\partial\alpha^{(i)}},\\
&\tilde\theta_2^{(i)} = \tfrac{\tilde q_2^{(i)}}{12G_{23}} - \tfrac{\tilde h^{(i)}}{6\tilde R^{(i)}}\tfrac{\partial\tilde\gamma_3^{(i)}}{\partial\beta^{(i)}}, && \tilde\varphi_2^{(i)} = \tfrac{{m_2}^{(i)} - \tilde Q_2^{(i)}}{10\tilde h^{(i)}\tilde G_{23}^{(i)}} - \tfrac{\tilde h^{(i)}}{\tilde R^{(i)}}\tfrac{\partial\tilde\theta_3^{(i)}}{\partial\beta^{(i)}},\\
&\tilde\gamma_3^{(i)} = \tfrac{1}{2\tilde h^{(i)}}\tfrac{\tilde T_0^{(i)}}{\tilde E_z^{(i)}} - \tfrac{1}{2}\left(\mu_1\varepsilon_1^{(i)} + \mu_2^{(i)}\varepsilon_2^{(i)}\right), && \tilde\theta_3^{(i)} = \tfrac{1}{\tilde h^{(i)}}\tfrac{\tilde M_0^{(i)}}{\tilde E_z^{(i)}} - \tfrac{1}{6}\left(\mu_1\eta_1^{(i)} + \mu_2\eta_2^{(i)}\right)
\end{aligned}
\tag{8}
$$

The same transformation for Paliy-Spiro theory gives:

$$
\begin{array}{l}
\tilde{T}_1^{(i)} = E_{11}\tilde{h}^{(i)}\varepsilon_1^{(i)} + E_{12}\tilde{h}^{(i)}\varepsilon_2^{(i)} + \frac{\tilde{h}^{(i)}}{12}((K_{11}-K_{12})\tilde{\eta}_1^{(i)} - K_{13}\tilde{\eta}_2^{(i)}) + \mu_1^{(i)}\frac{q_3^i}{2}\tilde{h}^{(i)},\\
\tilde{T}_2^{(i)} = E_{12}\tilde{h}^{(i)}\varepsilon_1^{(i)} + E_{22}\tilde{h}^{(i)}\varepsilon_2^{(i)} + \frac{\tilde{h}^{(i)}}{12}((K_{21}-K_{22})\tilde{\eta}_2^{(i)} - K_{23}\tilde{\eta}_1^{(i)}) + \mu_2^{(i)}\frac{q_3^i}{2}\tilde{h}^{(i)},\\
\tilde{T}_{12}^{(i)} = \tilde{G}_{12}^{(i)}\tilde{h}^{(i)}\left(\tilde{\omega}_1^{(i)} + \tilde{\omega}_2^{(i)} - \frac{(\tilde{h}^{(i)})^2}{12}\tilde{\tau}_1^{(i)}\right),\\
\tilde{T}_{21}^{(i)} = \tilde{G}_{12}^{(i)}\tilde{h}^{(i)}\left(\tilde{\omega}_1^{(i)} + \tilde{\omega}_2^{(i)} + \frac{(\tilde{h}^{(i)})^2}{12}\tilde{\tau}_2^{(i)}\right),\\
\tilde{M}_1^{(i)} = \frac{\tilde{h}^{(i)}}{6}(E_{11}\eta_1^{(i)} + E_{12}\eta_2^{(i)} + (K_{11}-K_{12})\tilde{\varepsilon}_1^{(i)} - K_{23}\tilde{\varepsilon}_2^{(i)}) + \mu_1^{(i)}\frac{q_3^i}{8}\tilde{h}^{(i)},\\
\tilde{M}_2^{(i)} = \frac{\tilde{h}^{(i)}}{6}(E_{12}\eta_1^{(i)} + E_{22}\eta_2^{(i)} + (K_{21}-K_{22})\tilde{\varepsilon}_2^{(i)} - K_{13}\tilde{\varepsilon}_1^{(i)}) + \mu_2^{(i)}\frac{q_3^i}{8}\tilde{h}^{(i)},\\
\tilde{M}_{12}^{(i)} = \tilde{G}_{12}^{(i)}\frac{\tilde{h}^{(i)}}{12}\left(\tilde{\tau}_1^{(i)} + \tilde{\tau}_2^{(i)} - (\tilde{h}^{(i)})^2\tilde{\omega}_1^{(i)}\right),\\
\tilde{M}_{21}^{(i)} = \tilde{G}_{12}^{(i)}\frac{\tilde{h}^{(i)}}{12}\left(\tilde{\tau}_1^{(i)} + \tilde{\tau}_2^{(i)} + (\tilde{h}^{(i)})^2\tilde{\omega}_2^{(i)}\right),\\
\tilde{Q}_1^{(i)} = \tilde{G}_{13}^{(i)}\tilde{h}^{(i)}\gamma_1^{(i)}, \qquad \tilde{Q}_2^{(i)} = \tilde{G}_{23}^{(i)}\tilde{h}^{(i)}\gamma_2^{(i)},\\
\sigma_{33} = \frac{\tilde{P}out_3{}^{(i)}\left(1+\frac{\tilde{h}^{(i)}}{2}\right)\left(0.5+\frac{z}{h^{(i)}}\right) - \tilde{P}in_3{}^{(i)}\left(1-\frac{\tilde{h}^{(i)}}{2}\right)\left(0.5-\frac{z}{h^{(i)}}\right)}{1+\frac{z}{R^{(i)}}},\\
\tilde{F}(\alpha,\beta,z)^{(i)} = \int\limits_0^z \frac{\sigma_{33}}{E_z}dz - (\mu_1\varepsilon_1 + \mu_2\varepsilon_2)z - \left[\mu_1\left(\eta_1 - \frac{\varepsilon_1}{R^{(i)}}\right) + \mu_2\eta_2\right]\frac{z^2}{2} + \left(\frac{\mu_1\eta_1}{R^{(i)}}\right)\frac{z^3}{3}.
\end{array}
\tag{9}
$$

By using Table 1 we obtain moments and strains as functions of the displacement $u, v, w, \gamma_1, \gamma_2$. By substituting these relations into equilibrium equation of the cylindrical shell

$$
\begin{array}{l}
\frac{\partial \tilde{T}_1^{(i)}}{\partial \alpha^{(i)}} + \tilde{R}^{(i)}\frac{\partial \tilde{T}_{21}^{(i)}}{\partial \beta^{(i)}} + \tilde{Q}_1^{(i)} + \tilde{q}_1^{(i)} = 0, \quad \frac{\partial \tilde{T}_{12}^{(i)}}{\partial \alpha^{(i)}} + \tilde{R}^{(i)}\frac{\partial \tilde{T}_2^{(i)}}{\partial \beta^{(i)}} + \tilde{q}_2^{(i)} = 0,\\
\frac{\partial \tilde{Q}_1^{(i)}}{\partial \alpha^{(i)}} + \tilde{R}^{(i)}\frac{\partial \tilde{Q}_2^{(i)}}{\partial \beta^{(i)}} - \tilde{T}_1^{(i)} + \tilde{q}_3^{(i)} = 0,\\
\frac{1}{\tilde{h}^{(i)}}\left(\frac{\partial \tilde{M}_1^{(i)}}{\partial \alpha^{(i)}} + \tilde{R}^{(i)}\frac{\partial \tilde{M}_{21}^{(i)}}{\partial \beta^{(i)}}\right) - \tilde{Q}_1^{(i)} + \tilde{m}_1^{(i)} = 0,\\
\frac{1}{\tilde{h}^{(i)}}\left(\frac{\partial \tilde{M}_{12}^{(i)}}{\partial \alpha^{(i)}} + \tilde{R}^{(i)}\frac{\partial \tilde{M}_2^{(i)}}{\partial \beta^{(i)}}\right) - \tilde{Q}_2^{(i)} + \tilde{m}_2^{(i)} = 0
\end{array}
\tag{10}
$$

one can get a system of five partial differential equations with five unknown functions for both theories. For the Rodionova-Titaev-Chernykh theory this system of equations is 14 order, and for the Paliy-Spiro theory is of 10 order. Substituting corresponding components of the deformation in formulas (1)-(3) one can get all components of the stress-deformed state of the shells under consideration.

4 TIMOSHENKO-REISSNER THEORY

In the first approximation the nanotube could be considered as a beam. If we use the Timoshenko-Reissner theory then the solution for beams with the freely supported edges has the following [6] form

$$
w(L_v) = \frac{F L_v{}^2 (L-L_v)^2}{3LEJ}\left(1 + \frac{1}{GS}\frac{3nEJ}{L_v(L-L_v)}\right). \tag{11}
$$

where L_v is a coordinate of the load application, $J = \frac{\pi R^4}{4}$ is moment of inertia for circular cross-section, $n = 5/6$ is coefficient in the formula Zhuravsky, $S = \pi R^2$ is cross-sectional area.

5 NUMERICAL METHOD

For solving the system of equations (10) in the displacements we will use the following series:

$$\begin{array}{lll} (u^{(i)}(\alpha,\beta)),(\gamma_1^{(i)}(\alpha,\beta)) & = & \sum_{n=0}^{\infty}\sum_{m=0}^{\infty}(u_{nm}^{(i)}),(\gamma 1_{nm}^{(i)})\sin[n\alpha]\sin[\bar{m}\beta], \\ (v^{(i)}(\alpha,\beta)),(\gamma_2^{(i)}(\alpha,\beta)) & = & \sum_{n=0}^{\infty}\sum_{m=0}^{\infty}(v_{nm}^{(i)}),(\gamma 2_{nm}^{(i)})\cos[n\alpha]\cos[\bar{m}\beta], \\ w^{(i)}(\alpha,\beta) & = & \sum_{n=0}^{\infty}\sum_{m=0}^{\infty} w_{nm}^{(i)}\cos[n\alpha]\sin[\bar{m}\beta], \qquad \bar{m}=(\pi m)/L, \end{array} \tag{12}$$

These formulas take into account the symmetry of the shell deformation in regard to plane $\alpha = 0$ and provide zero displacements u, γ_1 and w while $\beta = 0, L$. Expressions for v, γ_2 do not satisfy zero boundary conditions but this displacements are small. External and internal forces, which act on the shell surface can be represented as a product of sectional forces expanded in series. Let $X1_{mn}^{(i+1)}, X2_{mn}^{(i+1)}, X3_{mn}^{(i+1)}$ — be components of the pressure on the external surface of i^{th} shell, and $X1_{mn}^{(i)}, X2_{mn}^{(i)}, X3_{mn}^{(i)}$ pressure on its internal surface. Then expressions for the load and moments become:

$$\begin{array}{l} \tilde{m}_1^{(i)}(\alpha,\beta) = \sum_{n=0}^{\infty}\sum_{m=0}^{\infty}\frac{\tilde{h}^{(i)}}{2}\left(X1_{nm}^{(i+1)}\left(1+\frac{\tilde{h}^{(i)}}{2}\right)+X1_{nm}^{(i)}\left(1-\frac{\tilde{h}^{(i)}}{2}\right)\right)\sin[n\alpha]\sin[\bar{m}\beta], \\ \tilde{q}_1^{(i)}(\alpha,\beta) = \sum_{n=0}^{\infty}\sum_{m=0}^{\infty}\left(X1_{nm}^{(i+1)}\left(1+\frac{\tilde{h}^{(i)}}{2}\right)-X1_{nm}^{(i)}\left(1-\frac{\tilde{h}^{(i)}}{2}\right)\right)\sin[n\alpha]\sin[\bar{m}\beta], \\ \tilde{m}_2^{(i)}(\alpha,\beta) = \sum_{n=0}^{\infty}\sum_{m=0}^{\infty}\frac{\tilde{h}^{(i)}}{2}\left(X1_{nm}^{(i+1)}\left(1+\frac{\tilde{h}^{(i)}}{2}\right)+X1_{nm}^{(i)}\left(1-\frac{\tilde{h}^{(i)}}{2}\right)\right)\cos[n\alpha]\cos[\bar{m}\beta], \\ \tilde{q}_2^{(i)}(\alpha,\beta) = \sum_{n=0}^{\infty}\sum_{m=0}^{\infty}\left(X1_{nm}^{(i+1)}\left(1+\frac{\tilde{h}^{(i)}}{2}\right)-X1_{nm}^{(i)}\left(1-\frac{\tilde{h}^{(i)}}{2}\right)\right)\cos[n\alpha]\cos[\bar{m}\beta], \\ \tilde{m}_3^{(i)}(\alpha,\beta) = \sum_{n=0}^{\infty}\sum_{m=0}^{\infty}\frac{\tilde{h}^{(i)}}{2}\left(X1_{nm}^{(i+1)}\left(1+\frac{\tilde{h}^{(i)}}{2}\right)+X1_{nm}^{(i)}\left(1-\frac{\tilde{h}^{(i)}}{2}\right)\right)\cos[n\alpha]\sin[\bar{m}\beta], \\ q_3^{(i)}(\alpha,\beta) = \sum_{n=0}^{\infty}\sum_{m=0}^{\infty}\left(X1_{nm}^{(i+1)}\left(1+\frac{\tilde{h}^{(i)}}{2}\right)-X1_{nm}^{(i)}\left(1-\frac{\tilde{h}^{(i)}}{2}\right)\right)\cos[n\alpha]\sin[\bar{m}\beta] \end{array} \tag{13}$$

Index $i = 1$ corresponds to the internal, and $i = N+1$ to the external surface of the tube, which consists of N layers. Following [4], we accept the condition of rigidly bound layers:

$$\tilde{u}_k^{(i)}(\alpha,\beta,h/2) \;=\; \tilde{u}_k^{(i+1)}(\alpha,\beta,-h/2), \qquad k=1,2,3 \tag{14}$$

The load localized in a small rectangular area can be represented in the form of a product of the Fourier series of two loading functions in cross-section and longitudinal section:

$$Pa[\alpha] = P(\frac{C}{L}+\frac{2}{L}\sum_{n=0}^{\infty}\frac{L}{n\pi}\sin(\frac{n\pi}{L}C)\cos(\frac{n\pi}{L}\alpha)) \tag{15}$$

Pressure in longitudinal section of the tube is equal to

$$Pb[\beta] = P(\frac{4}{L}\sum_{m=0}^{\infty}\frac{L}{m\pi}\sin(\frac{m\pi}{L}C)sin(\frac{m\pi}{L}L_v)\sin(\frac{m\pi}{L}\beta)), \tag{16}$$

where L_v is a center of load application, $2C$ is a size of load application area, P is pressure in the area. Pressure area is described by function of the product of the series:

$$Pd[\alpha,\beta] = Pa[\alpha] * Pb[\beta] \tag{17}$$

The load is applied to the outer surface of the tube:

$$X1_{nm}^{(N+1)} = 0, \quad X2_{nm}^{(N+1)} = 0, \quad X3_{nm}^{(N+1)} = Pd[\alpha,\beta] \tag{18}$$

Pressure on the internal surface of the tube is absent:

$$X1_{nm}^{(1)} = 0, \quad X2_{nm}^{(1)} = 0, \quad X3_{nm}^{(1)} = 0 \tag{19}$$

Substituting dependencies (11),(12) and (16) in the system (10) and in conditions (13) we obtain a system of $8N-3$ linear algebraic equations for $5N$ deformation components and $3N-3$ forces of interaction between layers of shells. Each of the obtained coefficients $u_{nm}^{(i)}$, $v_{nm}^{(i)}$, $w_{nm}^{(i)}$, $\gamma 1_{nm}^{(i)}$, $\gamma 2_{nm}^{(i)}$, $X1_{mn}^{(i)}$, $X2_{mn}^{(i)}$, $X3_{mn}^{(i)}$ is a member of the Fourier series of functions of deformation and loading functions.

For realization of the aforementioned numerical method we developed a program based on code Mathematica 7.0.

6 NUMERICAL RESULTS

In [4] deformation of a nanotube was considered with the following parameters: thickness of each of the 100 layers $h = 0,135$ nm, inner tube radius R=2.5 nm, outer R=16 nm, length of the tube L=500 nm. For values of the modulus of elasticity of the shell $E_{1,2,3} = 1.75 * 10^{11}$ Pa, and relatively small value of the shear modulus $G_{13} = G_{12} = G_{23} = 2.3 * 10^7$ Pa. Poisson ratios $\nu_{12} = \nu_{21} = \nu_{32} = \nu_{31} = \nu_{23} = \nu_{13} = 0.3$.

The table 2 shows the values of deflection of the described tube, obtained by RTCH, TR theory and theory of PS. Calculation of the functions of displacement was done with external force $F_v = 10$ nN. The area of applied load is $[40 * 40]$ nm^2. For comparison we present values of deflections of a transversal-isotropic tube, which were received in code Ansys 11 where 3-dimensional 20 knots element Solid 186 was used. Lines ”TR1”, ”Ansys1” correspond to tube with a hole; lines ”TR2”, ”Ansys2” correspond to solid tube.

L_v	250	220	200	170	150	120	100	70	40
TR1	60.61	59.7	58.07	54.14	50.52	43.65	38.12	28.47	17.24
TR2	59.2	58.31	56.72	52.87	49.34	42.62	37.22	27.79	16.82
RTCH	57.79	56.86	55.21	51.22	47.56	40.62	35.07	25.45	14.4
PS	57.54	56.62	54.97	51	47.35	40.45	34.92	25.34	14.34
Ansys1	54.11	53.26	51.7	48.3	45.1	39.02	34.07	25.37	15.37
Ansys2	52.39	52.38	50.12	46.77	43.71	37.81	33.02	24.6	14.91

Table 2: Deflection of the many-layer nanotube.

Let us compare results obtained by the three-dimensional theory that is used in code Ansys 11 with results obtained by the aforementioned non-classical theories of shells for single-layer cylindrical shell. We consider a shell with constant outer radius and gradually increase the thickness of the shell (and consequently reduce a radius of the middle surface of the shell). The following table lists the values of deflections at the center of considered shells.

Figures 2 present functions of the upper layer displacement of the shell when the load is applied to the center of the tube.

Table 3 gives the values of the deflections of shells. Other values that characterize the stress-strain state of shells are also similar. With increasing the relative thickness of the shell, values of deflection obtained with the PS theory are closer to the values obtained with the finite element method.

h/R	1/15	1/10	1/5	1/4	1/3	1/2
TR1	46.33	31.91	17.55	14.71	11.88	9.13
RTCH	78.09	52.64	27.14	22.13	17.31	12.98
PS	75.28	49.82	24.29	19.26	14.39	9.9
Ansys1	76.36	46.44	20.37	15.9	11.95	8.92

Table 3: Deflection of a single-layer shell with constant outer radius

REFERENCES

[1] A.V. Ankudinov, S.M. Bauer, S.V. Kashtanova, N.F. Morozov, I.A. Nyapshaev, Study of mechanical stiffness of a solitary asbestos nanotub. *Bulletin of Higher Educational Institutions. The North Caucasus Region.* Series Natural Sciences 7-9 (2009).

[2] A.V. Ankudinov, S.M. Bauer, A.M. Ermakov, S.V. Kashtanova, N.F. Morozov, On mechanical properties of asbestos nanotubes. *XIV International Conference Modern Problems of the Mechanics of Solid Media*. Azov, Russia, 2010. Conference Proceedings, Vol. 1, Pp. 35-38.

[3] A.M. Krivtsov, N.F. Morozov, Anomalies in the mechanical properties of nano sized objects, *Dokl. Akad. Nauk*, 381 (3), 345-347 (2001).

[4] V.A. Rodionova, B.F. Titaev, K.F Chernykh, *Applied Theory of Anisotropic Plates and Shells*. St. Peterburg University Press, St. Petersburg (1996) (in Russian).

[5] O.M. Paliy, V.E. Spiro, *Anisotropic Shells in Shipbuilding. Theory and Analysis*. Sudostroenie, Leningrad (1977) (in Russian).

[6] L.H. Donnell, *Beams, Plates and Shells*. McGraw-Hill Book Company, 1976.

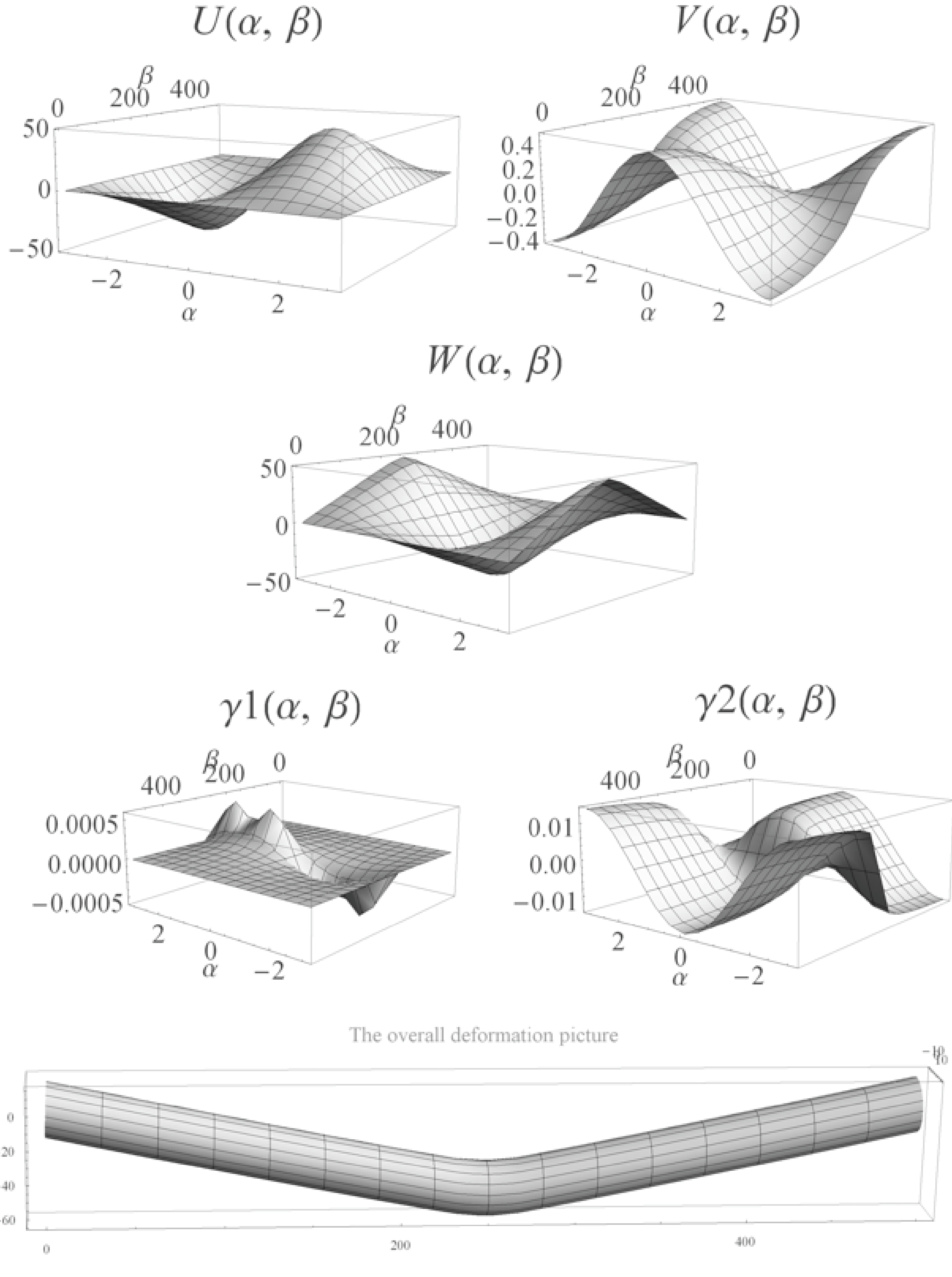

Figure 2: Deformed tube